SUPPLEMENTARY INFORMATION: PREDICTING DEFECT BEHAVIORS IN B2 INTERMETALLICS BY MERGING *AB INITIO* MODELING AND MACHINE LEARNING

BHARAT MEDASANI, ANTHONY GAMST, HONG DING, WEI CHEN, KRISTIN A. PERSSON, MARK ASTA, ANDREW CANNING, AND MACIEJ HARANCZYK

1. Data Tables supporting the text in the article

Table 1. Mann-Whitney-Wilcoxon rank sum statistic (p-value) for all the descriptors considered. Smaller p-value indicates higher predictive power.

Atomic Property	Symbol	p-value			
		Min.	Max.	Avg.	Diff.
Group		0.366	0.003	0.224	0.008
Principle quantum number	n	—	0.009	0.0361	0.474
Atomic number	Z	0.253	0.007	0.011	0.282
Effective nuclear charge [1]	Z_{eff}	0.727	0.015	0.284	0.296
Electronegativity (Pauling) [2]	X	0.021	0.090	0.844	0.020
Electronegativity (Mulliken) [3]	X_{abs}	0.004	0.024	0.625	0.165
Electronegativity (Allred) [4]	X_A	0.015	0.540	0.152	0.007
Electron density at Wigner Seitz cell boundary [5]	$n_{WS}^{1/3}$	0.0005	0.417	0.012	0.006
Atomic Radius	R	0.950	0.067	0.170	0.037
Zunger pseudopotential radii [6]	R_Z	0.839	0.027	0.107	0.156
Melting temperature	T_m	0.140	0.085	0.057	0.196
Hardness (absolute) [7, 3]	ν_{abs}	0.451	0.780	0.647	0.586
Transition metal flag	trans	—	—	0.637	0.637
Compound Property		p-value			
Density	ρ	0.682			
Formation energy per atom	ΔE_f	0.0002			
Volume per atom	V_0	0.012			

TABLE 2. Retained descriptors after Spearman correlation analysis.

Descriptor	Description
$\mathrm{Group_{min}}$	Minimum of group numbers
$\mathrm{Group_{max}}$	Maximum of group numbers
ΔGroup	Difference in group numbers
$\mathrm{n_{max}}$	Maximum of principle quantum numbers
Δn	Difference in principle quantum numbers
$\mathrm{Z_{min}}$	Minimum of atomic numbers
$\mathrm{Z_{max}}$	Maximum of atomic numbers
ΔZ	Difference in atomic numbers
$\mathrm{X_{min}}$	Minimum of Pauling electronegativities
$\mathrm{X_{max}}$	Maximum of Pauling electronegativities
ΔX	Difference in Pauling electronegativities
$\mathrm{X_{abs,min}}$	Minimum of Mulliken electronegativities
$\mathrm{X_{abs,max}}$	Maximum of Mulliken electronegativities
$\Delta\mathrm{X_{abs}}$	Difference in Mulliken electronegativities
$\mathrm{X}_{A,\mathrm{min}}$	Minimum of Allred electronegativities
$\mathrm{X}_{A,\mathrm{max}}$	Maximum of Allred electronegativities
$\Delta\mathrm{X}_A$	Difference in Allred electronegativities
$\mathrm{n_{WS,min}}$	Minimum of electron densities at WS cell boundaries
$\mathrm{n_{WS,max}}$	Maximum of electron densities at WS cell boundaries
$\Delta\mathrm{n_{WS}}$	Difference in electron densities at WS cell boundaries
$\mathrm{R_{min}}$	Minimum of atomic radii
$\mathrm{R_{max}}$	Maximum of atomic radii
ΔR	Difference in atomic radii
$\mathrm{R}_{Z,\mathrm{min}}$	Minimum of Zunger pseudopotential radii
$\mathrm{R}_{Z,\mathrm{max}}$	Maximum of Zunger pseudopotential radii
$\Delta\mathrm{R}_Z$	Difference in Zunger pseudopotential radii
$\mathrm{T_{m,min}}$	Minimum of melting temperatures
$\mathrm{T_{m,max}}$	Maximum of melting temperatures
$\Delta\mathrm{T_m}$	Difference in melting temperatures
$\nu_{\mathrm{abs,min}}$	Minimum of absolute hardness
$\nu_{\mathrm{abs,max}}$	Maximum of absolute hardness
$\Delta\nu_{\mathrm{abs}}$	Difference in absolute hardness
ρ	density
ΔE_f	Formation energy per atom
$\mathrm{V_0}$	Volume per atom

TABLE 3. B2 compounds for which the point defect concentrations were computed and the corresponding values of the descriptors retained in reduced MART model. The third column ΔE_f represents the formation energy, defined as $\Delta E_f = E_{AB} - (E_A + E_B)/2$, where E_{AB}, E_A and E_B are the energies per atom of the AB B2 intermetallic compounds, and the pure elements (A and B) in their equilibrium crystal structure. In the column of defect type classification (DTC), the value of 0 indicates the intermetallic compound belongs to antisite dominant type while the value of 1 indicates it belongs to non-antisite dominant type.

	Formula	ΔE_f	$\Delta n_{WS}^{1/3}$	ΔR_Z	$Z_{\max}$	$n_{WS,\min}^{1/3}$	$X_{A,\max}$	DTC
1	YCd	-0.354	1.21	0.563	48	1.21	1.46	0
2	ScCd	-0.294	1.24	0.431	48	1.24	1.46	0
3	CaHg	-0.554	0.91	0.436	80	0.91	1.44	1
4	FeCo	-0.057	1.75	0.087	27	1.75	1.70	0
5	HfRu	-0.823	1.43	0.221	72	1.43	1.42	1
6	AlRh	-1.093	1.39	0.806	45	1.39	1.47	1
7	CaPd	-0.681	0.91	0.404	46	0.91	1.35	1
8	ScZn	-0.376	1.27	0.752	30	1.27	1.66	0
9	TiOs	-0.714	1.47	0.054	76	1.47	1.52	0
10	MgTl	-0.034	1.12	0.192	81	1.12	1.44	1
11	YRh	-0.851	1.21	0.308	45	1.21	1.45	1
12	SrTl	-0.429	0.84	0.716	81	0.84	1.44	1
13	YCu	-0.238	1.21	0.723	39	1.21	1.75	1
14	HfTc	-0.483	1.43	0.187	72	1.43	1.36	0
15	YIr	-0.788	1.21	0.224	77	1.21	1.55	1
16	ScCu	-0.278	1.27	0.593	29	1.27	1.75	1
17	VTc	-0.376	1.64	0.173	43	1.64	1.45	0
18	BaZn	-0.160	0.81	1.153	56	0.81	1.66	1
19	ZnAg	-0.043	1.32	0.465	47	1.32	1.66	0
20	AlRu	-0.672	1.39	0.869	44	1.39	1.47	0
21	LiHg	-0.372	0.98	0.796	80	0.98	1.44	1
22	FeRh	-0.049	1.76	0.354	45	1.76	1.64	0
23	ScIr	-1.035	1.27	0.091	77	1.27	1.55	1
24	MnV	-0.283	1.61	0.181	25	1.61	1.60	0
25	YHg	-0.509	1.21	0.396	80	1.21	1.44	1
26	MnRh	-0.185	1.61	0.253	45	1.61	1.60	0
27	CdAg	-0.059	1.24	0.139	48	1.24	1.46	0
28	ZnRh	-0.383	1.32	0.582	45	1.32	1.66	0
29	MgSc	-0.042	1.17	0.603	21	1.17	1.23	0

	Formula	ΔE_f	$\Delta n_{WS}^{1/3}$	ΔR_Z	$Z_{\max}$	$n_{WS,\min}^{1/3}$	$X_{A,\max}$	DTC
30	MnPd	-0.197	1.61	0.197	46	1.61	1.60	0
31	MgRh	-0.474	1.17	0.431	45	1.17	1.45	0
32	YAl	-0.414	1.21	1.096	39	1.21	1.47	1
33	ZnAu	-0.208	1.32	0.687	79	1.32	1.66	1
34	CaTl	-0.444	0.91	0.585	81	0.91	1.44	0
35	ScPd	-0.911	1.27	0.231	46	1.27	1.35	1
36	ZnCu	-0.086	1.32	0.163	30	1.32	1.75	0
37	ScHg	-0.429	1.24	0.264	80	1.24	1.44	0
38	MnZn	0.068	1.32	0.332	30	1.32	1.66	0
39	MnNi	-0.039	1.61	0.036	28	1.61	1.75	0
40	SrHg	-0.535	0.84	0.569	80	0.84	1.44	1
41	CaCd	-0.361	0.91	0.602	48	0.91	1.46	0
42	AlFe	-0.325	1.39	0.460	26	1.39	1.64	0
43	YAg	-0.336	1.21	0.425	47	1.21	1.42	0
44	MgAu	-0.609	1.17	0.537	79	1.17	1.42	1
45	ScAg	-0.285	1.27	0.293	47	1.27	1.42	0
46	ScAl	-0.448	1.27	0.972	21	1.27	1.47	1
47	ScRh	-1.036	1.27	0.175	45	1.27	1.45	1
48	TiRe	-0.396	1.47	0.076	75	1.47	1.46	0
49	AlOs	-0.399	1.39	0.902	76	1.39	1.52	0
50	YZn	-0.359	1.21	0.880	39	1.21	1.66	1
51	ScCo	-0.361	1.27	0.612	27	1.27	1.70	1
52	BaHg	-0.523	0.81	0.683	80	0.81	1.44	1
53	GaRh	-0.686	1.31	0.783	45	1.31	1.82	1
54	ZnNi	-0.238	1.32	0.296	30	1.32	1.75	1
55	AlNi	-0.659	1.39	0.524	28	1.39	1.75	1
56	HfOs	-0.711	1.43	0.187	76	1.43	1.52	1
57	HfRh	-0.865	1.43	0.287	72	1.43	1.45	0
58	ScNi	-0.508	1.27	0.462	28	1.27	1.75	1
59	BaCd	-0.322	0.81	0.845	56	0.81	1.46	1
60	SrMg	-0.058	0.84	0.901	38	0.84	1.23	0
61	YMg	-0.109	1.17	0.732	39	1.17	1.23	0
62	TiCo	-0.383	1.47	0.487	27	1.47	1.70	0
63	AlPd	-0.878	1.39	0.752	46	1.39	1.47	1
64	TiRu	-0.765	1.47	0.019	44	1.47	1.42	0
65	MgAg	-0.252	1.17	0.313	47	1.17	1.42	0
66	ScRu	-0.546	1.27	0.108	44	1.27	1.42	0
67	MgHg	-0.219	1.17	0.342	80	1.17	1.44	1

	Formula	ΔE_f	$\Delta n_{WS}^{1/3}$	ΔR_Z	$Z_{\max}$	$n_{WS,\min}^{1/3}$	$X_{A,\max}$	DTC
68	ScAu	-0.808	1.27	0.067	79	1.27	1.42	0
69	InRh	-0.431	1.17	0.411	49	1.17	1.49	1
70	ZrZn	-0.278	1.32	0.803	40	1.32	1.66	0
71	RbAu	-0.280	0.60	0.852	79	0.60	1.42	1
72	ScPt	-1.232	1.27	0.037	78	1.27	1.44	1
73	LiTl	-0.227	0.98	0.650	81	0.98	1.44	1
74	BeNi	-0.473	1.60	1.350	28	1.60	1.75	0
75	AlPt	-0.936	1.39	0.937	78	1.39	1.47	1
76	MgPd	-0.746	1.17	0.375	46	1.17	1.35	1
77	SrCd	-0.333	0.84	0.734	48	0.84	1.46	1
78	GaRu	-0.305	1.31	0.847	44	1.31	1.82	0
79	AlIr	-0.940	1.39	0.886	77	1.39	1.55	1
80	ZrOs	-0.529	1.39	0.128	76	1.39	1.52	1
81	VOs	-0.240	1.64	0.173	76	1.64	1.52	0
82	MnAu	0.130	1.57	0.361	79	1.57	1.60	0
83	YAu	-0.858	1.21	0.200	79	1.21	1.42	1
84	GaCo	-0.277	1.31	0.350	31	1.31	1.82	1
85	MnHg	0.335	1.24	0.164	80	1.24	1.60	1
86	HfCo	-0.389	1.43	0.722	72	1.43	1.70	1
87	CdAu	-0.173	1.24	0.365	79	1.24	1.46	1
88	TiFe	-0.413	1.47	0.401	26	1.47	1.64	1
89	BeCu	-0.105	1.47	1.231	29	1.47	1.75	0
90	TaTc	-0.500	1.63	0.103	73	1.63	1.36	0
91	TiTc	-0.493	1.47	0.054	43	1.47	1.36	0
92	YTl	-0.370	1.12	0.545	81	1.12	1.44	0
93	AlCo	-0.603	1.39	0.373	27	1.39	1.70	1
94	BePd	-0.596	1.60	1.552	46	1.60	1.47	1
95	BeRh	-0.616	1.60	1.600	45	1.60	1.47	0
96	TiBe	-0.143	1.47	1.639	22	1.47	1.47	0
97	ZrIr	-0.758	1.39	0.145	77	1.39	1.55	1
98	VFe	-0.123	1.64	0.282	26	1.64	1.64	0
99	LiAg	-0.222	0.98	0.768	47	0.98	1.42	0
100	LiPd	-0.426	0.98	0.828	46	0.98	1.35	0

TABLE 4. Compounds for which the predictions of the machine learning models do not agree with the DFT calculations.

Model	Compounds						
Decision Tree	LiAg	HfCo	ScAl	ScAu	GaCo	MgHg	ZnAu
	LiHg	**BePd**	TiFe	NiZn	AlRu	InRh	MgTl
	YAl	HfRh	ScRu	CdAu	MnHg		
f-MART	LiPd	LiAg	CaCd	**BePd**	TiFe	NiZn	
r-MART	**BePd**	AlRu					

TABLE 5. Comparison of the r-MART predictions against the DFT predictions for 14 B2 metal alloys which are not used in the fitting of the r-MART model.

Compound	DFT prediction	r-MART prediction	Agreement (Y/N)
BeAu	Non-antisite	Antisite	N
CuAu	Antisite	Antisite	Y
InHg	Non-antisite	Non-antisite	Y
KAu	Non-antisite	Non-antisite	Y
KNa	Antisite	Antisite	Y
LiCa	Antisite	Antisite	Y
LiMg	Antisite	Antisite	Y
LiSn	Non-antisite	Non-antisite	Y
MgGa	Antisite	Non-antisite	N
NaSr	Antisite	Antisite	Y
SnRu	Non-antisite	Non-antisite	Y
TaMo	Antisite	Antisite	Y
TaW	Antisite	Antisite	Y
ZrFe	Non-antisite	Antisite	N

TABLE 6. Influence of antiferromagnetic (AFM) versus ferromagnetic (FM) magnetic ordering on the predicted dominant defects type classification in 16 B2 intermetallic compounds for which FM spin-polarized calculations converged with significant magnetic moments. In the second column, E^{FM} and E^{AFM} denote the energies per atom for FM and AFM spin ordering, respectively. Among these 16 systems, 9 exhibited energetic preference for antiferromagnetic (AFM) ordering, but the energy differences between FM and AFM was found to be small, on the scale of the formation and defect energies (< 0.1 meV/atom), in 4 out of the 9 systems. The defect calculations were performed for the systems which exhibit preference towards AFM ordering with non-negligible energy difference (larger than 1 meV/atom). The dominant defect types did not change as a result of a change from FM to AFM magnetic configurations.

Compound	$E^{FM} - E^{AFM}$ (meV/atom)	Negligible	FM stable	AFM stable	FM Defect	AFM Defect
GaCo	0.06	*		*		
MnAu	46.78			*	Antisite	Antisite
MnHg	47.66			*	Non-antisite	Non-antisite
MnNi	-11.17		*			
MnPd	26.39			*	Antisite	Antisite
MnRh	-36.81		*			
MnV	0.13	*		*		
MnZn	17.76			*	Antisite	Antisite
ScCo	0.077	*		*		
TiCo	-5.99		*			
TiFe	0.084	*		*		
VFe	-31.58		*			
FeRh	22.88			*	Antisite	Antisite
AlFe	-0.48	*	*			
FeCo	-209.81		*			
AlCo	-0.17	*	*			

TABLE 7. Dominant defect type with respect to supercell size (in number of atoms). The five B2 compounds shown here are chosen such that they are on ground state hull and the atomic size difference between the constituent elements is greater than 0.25 Å to check the effect of strain-induced interactions. The results demonstrate that the supercell size does not alter the classification of these five compounds as antisite versus vacancy formers.

Compound	Defect Type			
(Supercell size =)	54	128	250	432
CaPd	Non-antisite	Non-antisite	Non-antisite	Non-antisite
ScPt	Non-antisite	Non-antisite	Non-antisite	Non-antisite
YCu	Non-antisite	Non-antisite	Non-antisite	Non-antisite
ScRu	Antisite	Antisite	Antisite	Antisite
RbAu	Non-antisite	Non-antisite	Non-antisite	Non-antisite

2. Classification of elements with electron density values at the Wigner-Seitz boundary

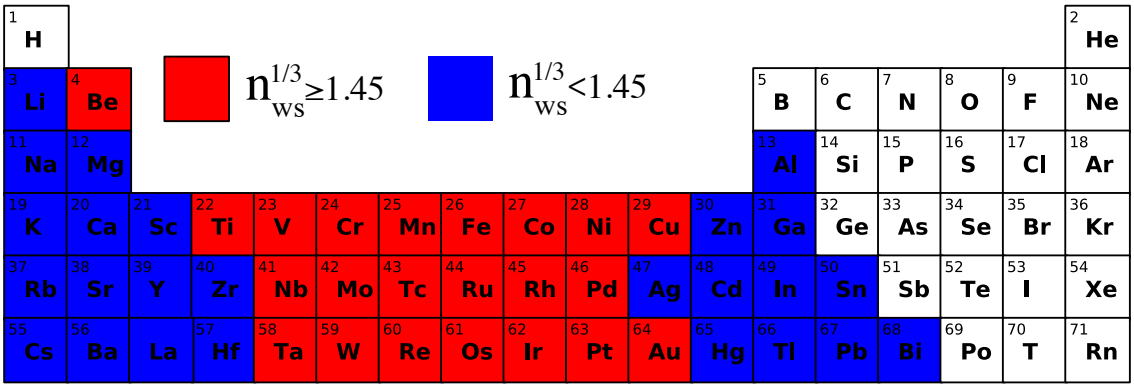

FIGURE S1. Classification of metallic elements in periodic table based on the electron density values at the Wigner-Seitz boundary ($n_{WS}^{1/3}$) from Ref. [5], where elements with $n_{WS}^{1/3} \geq 1.45$ are marked in red and the others are marked in blue. This classification is based on the division rule proposed by the simple decision tree model as shown in Fig. 4 of the manuscript.

3. Stability map of B2 intermetallics

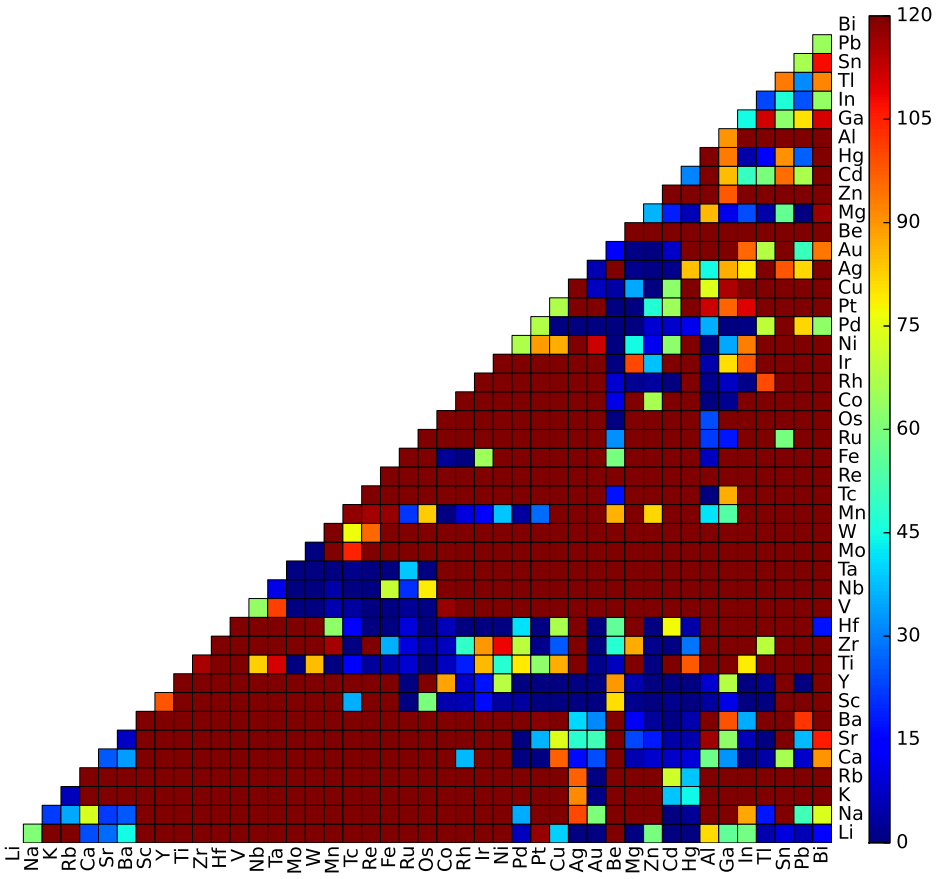

FIGURE S2. Stability map of B2 intermetallics as a function of energy above hull (in meV). The energy above hull for a compound is evaluated by comparing the energies of the computed entries to the predicted ground states in the Materials Project database [8]. For the visibility of stable compounds, the B2 intermetallics with energies above hull of greater than 120 meV/atom are plotted with a single color.

4. Supercell size dependency on defect concentration

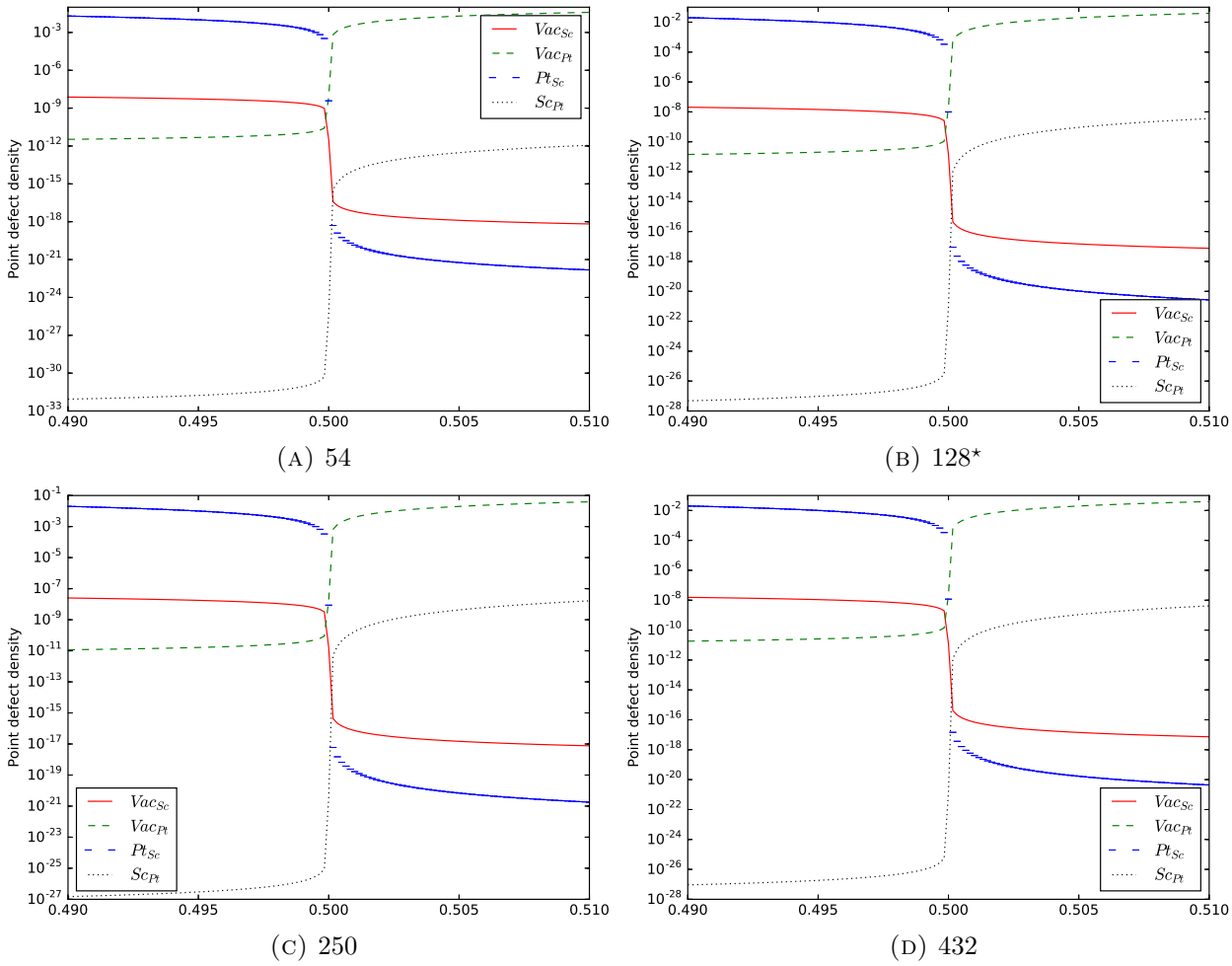

(A) 54 (B) 128* (C) 250 (D) 432

Figure S3. Defect concentrations in ScPt as a function of Sc mole fraction for different supercell sizes (in number of atoms).

References

[1] E. Clementi, D. L. Raimondi, Atomic screening constants from scf functions, The Journal of Chemical Physics 38 (11) (1963) 2686–2689. doi:http://dx.doi.org/10.1063/1.1733573.
URL `http://scitation.aip.org/content/aip/journal/jcp/38/11/10.1063/1.1733573`

[2] L. Pauling, The Nature of the Chemical Bond, 3rd Edition, Cornell University Press, Ithaca, New York, 1960.

[3] R. G. Pearson, Absolute electronegativity and hardness: application to inorganic chemistry, Inorganic Chemistry 27 (4) (1988) 734. arXiv:http://dx.doi.org/10.1021/ic00277a030, doi:10.1021/ic00277a030.
URL http://dx.doi.org/10.1021/ic00277a030

[4] A. Allred, Electronegativity values from thermochemical data, Journal of Inorganic and Nuclear Chemistry 17 (34) (1961) 215. doi:http://dx.doi.org/10.1016/0022-1902(61)80142-5.
URL http://www.sciencedirect.com/science/article/pii/0022190261801425

[5] A. R. Miedema, R. Boom, F. R. D. Boer, On the heat of formation of solid alloys, J. Less-Common Met. 41 (1975) 283.

[6] A. Zunger, Systematization of the stable crystal structure of all AB-type binary compounds: A pseudopotential orbital-radii approach, Phys. Rev. B 22 (1980) 5839–5872. doi:10.1103/PhysRevB.22.5839.
URL http://link.aps.org/doi/10.1103/PhysRevB.22.5839

[7] R. G. Parr, R. G. Pearson, Absolute hardness: companion parameter to absolute electronegativity, Journal of the American Chemical Society 105 (26) (1983) 7512–7516. arXiv:http://dx.doi.org/10.1021/ja00364a005, doi:10.1021/ja00364a005.
URL http://dx.doi.org/10.1021/ja00364a005

[8] A. Jain, S. P. Ong, G. Hautier, W. Chen, W. D. Richards, S. Dacek, S. Cholia, D. Gunter, D. Skinner, G. Ceder, K. a. Persson, APL Materials 1 (1) (2013) 011002. doi:10.1063/1.4812323.